

Tu 11 16

## Efficient 3D MT Inversion Using Finite-difference Time-domain Modelling

S. de la Kethulle de Ryhove\* (Electromagnetic Geoservices ASA), J.P. Morten (Electromagnetic Geoservices ASA) & K. Kumar (Electromagnetic Geoservices ASA)

### SUMMARY

---

We show how a finite-difference time-domain modelling algorithm can be utilised for efficient 3D inversion of marine magnetotelluric (MT) data, and demonstrate the capability of our inversion on a synthetic salt dome. In comparison to frequency-domain modelling methods which are typically applied, two advantages of the finite-difference time-domain modelling method are (1) that it is an explicit, low-memory method; and (2) that it allows forward and adjoint computation for the electromagnetic field unknowns at all frequencies of interest in a single modelling run.

## Introduction

The most popular methods for numerical 3D magnetotelluric (MT) forward modelling can be divided into three main categories: finite-difference methods, finite-element methods, and integral equation methods. Authors utilising these methods to develop algorithms for solving the MT forward problem (Mackie et al., 1993; Hursan and Zhdanov, 2002; Farquharson and Miensopust, 2011) typically start from a frequency-domain formulation of Maxwell's equations. Discretising the spatial derivatives then leads, for each frequency of interest, to a system of linear equations which must be solved to obtain the unknown electromagnetic field values.

We propose to compute MT responses using the finite-difference time-domain (FDTD) method, directly solving Maxwell's equations in the time-domain. An obvious advantage of this approach is that the FDTD method is an explicit method with low memory requirements, and does not require the solution of systems of linear equations. Using even the simplest iterative solvers (see e.g. Sleijpen and Fokkema (1993), table 3.1) with a finite-difference frequency-domain method leads to memory requirements that are significantly higher than those of the FDTD method. A second advantage is that a single FDTD simulation allows to compute the electromagnetic field unknowns at all frequencies of interest, as opposed to frequency-domain methods which must usually be run once for each frequency of interest.

We developed a numerically efficient algorithm for 3D inversion of marine MT data using our FDTD MT modelling approach. In this paper, we first describe the main ideas behind our modelling algorithm, and subsequently show how the scheme is utilised in 3D inversion. To demonstrate the performance of our implementation, we consider unconstrained inversion of data from a synthetic salt dome model (see Figure 1). We also compare forward modelling responses to results obtained using integral equation software to demonstrate the accuracy of our modelling approach.

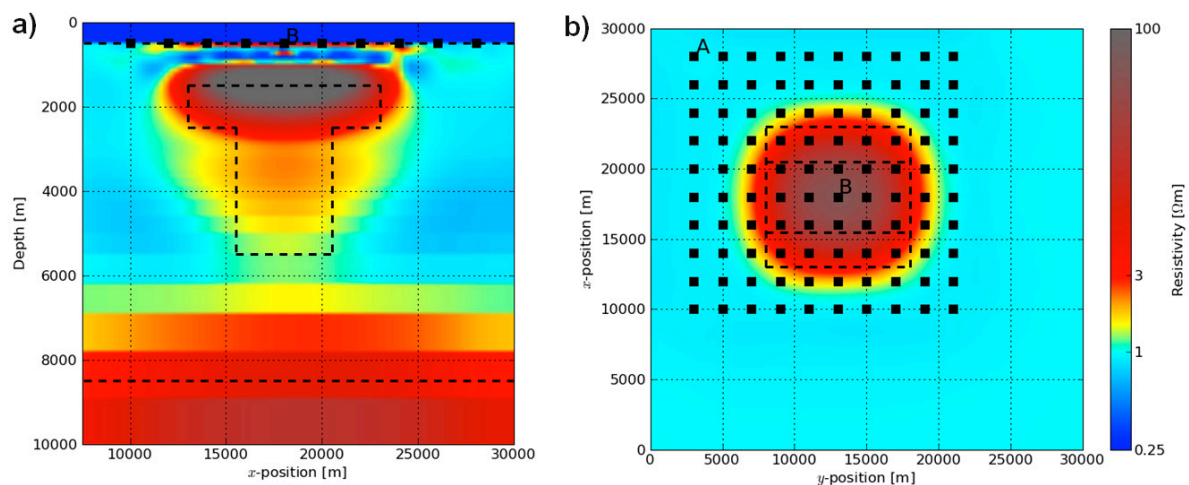


**Figure 1** This figure shows the inverted salt dome model, and the thick dashed lines show the outlines for the corresponding geometries in the true model. The grey squares indicate receiver positions. Note that the maximum resistivity in the model exceeds the maximum range of the colour scale. Panel (a) shows a vertical cross section at  $x = 13000$  m, and panel (b) shows a plan view at depth 2000 m.

## Time-domain modelling for MT responses

Our FDTD modelling algorithm is described in detail in (de la Kethulle de Ryhove and Mittet, 2012). In this section, we limit ourselves to a discussion of the main ideas. Let  $\mathbf{E}$  and  $\mathbf{H}$  denote the electric and magnetic fields,  $\mathbf{J}$  and  $\mathbf{K}$  denote the electric and magnetic current densities of external sources,  $\sigma$  denote the electrical conductivity tensor (assumed to be diagonal), and  $\mu_0 = 4\pi \times 10^{-7}$  H/m denote the magnetic permeability of free space. In the low-frequency limit relevant for magnetotelluric exploration,

the physical problem of interest can then be modelled by using the relations

$$\nabla \times \mathbf{E} = -\mu_0 \partial_t \mathbf{H} - \mathbf{K}, \quad (1)$$

$$\nabla \times \mathbf{H} = \sigma \mathbf{E} + \mathbf{J}. \quad (2)$$

The main idea behind our algorithm is to apply Yee's (1996) original FDTD scheme to equations (1) and (2) to compute the necessary electromagnetic fields. There are, however, some challenges. These include the wide range of propagation velocities and the implementation of boundary conditions. We address these two challenges below.

In the low-frequency regime relevant for geophysical problems, one difficulty regarding the use of the FDTD method is the wide range of propagation velocities. For a given grid spacing, the highest propagation velocity limits the maximum allowed step length in time  $\Delta t$  via a stability criterion. However, one must wait for all significant events affecting the components of the signal propagating at the lowest propagation velocities to have taken place before the computation can be stopped. This can lead to very long simulation times. One way to reduce the computation time is to use a mathematical transformation to convert the physical problem to one where the range of propagation velocities is reduced as suggested by Maaø (2007) and Mittet (2010). Following for example (Mittet, 2010), one then introduces a fictitious electric permittivity tensor  $\epsilon' = \frac{\sigma}{2\omega_0}$ , with  $\omega_0 \in \mathbb{R}^+$  an arbitrary parameter, and Yee's time marching scheme is actually applied in the so-called *fictitious time domain* to the relations

$$\nabla \times \mathbf{E}' = -\mu_0 \partial_{t'} \mathbf{H}' - \mathbf{K}', \quad (3)$$

$$\nabla \times \mathbf{H}' = \epsilon' \partial_{t'} \mathbf{E}' + \mathbf{J}', \quad (4)$$

where  $\mathbf{E}'$ ,  $\mathbf{H}'$ ,  $\mathbf{J}'$ , and  $\mathbf{K}'$  are fictitious time domain quantities that are related to the quantities  $\mathbf{E}$ ,  $\mathbf{H}$ ,  $\mathbf{J}$ , and  $\mathbf{K}$  from equations (1) and (2) (Mittet, 2010).

Let us now discuss the treatment of boundary conditions when using an FDTD method on a computational domain  $\Omega \subset \mathbb{R}^3$ , with a Yee grid  $\Omega_N$  consisting of a Cartesian product of one-dimensional grids. In order to compute the required spatial finite-differences centred around a node that is located on one of the outermost planes of  $\Omega_N$ , knowledge of field values for "ghost" nodes that do not belong to  $\Omega_N$  is required. Such knowledge is by definition not available in the FDTD scheme. This difficulty can be addressed by extending the computational domain  $\Omega$  with a medium which absorbs perfectly all waves propagating outwards from  $\Omega$ , effectively simulating its extension to infinity. One can then simply set the field values at the ghost nodes to zero without introducing any errors. For FDTD schemes, the convolutional perfectly matched layer (CPML) introduced in Roden and Gedney (2000) is a very powerful implementation of the so-called *absorbing boundary conditions* (ABCs) described above. The absorption properties of a CPML for direction  $\xi$ , extending from  $\xi = 0$  to  $\xi = \delta_\xi$ , are determined by the complex stretching variable

$$s_\xi(u, \omega') = \alpha_\xi(u) + \frac{\sigma_\xi(u)}{\tau_\xi(u) - i\omega'}, \quad (5)$$

where  $\xi$  is one of  $\{x, y, z\}$ ,  $0 \leq u \leq \delta_\xi$ ,  $\omega'$  denotes angular frequency, and the real functions  $\alpha_\xi(u)$ ,  $\sigma_\xi(u)$ , and  $\tau_\xi(u)$  must be designed appropriately for the resulting CPML to exhibit the desirable absorption properties. Our specific choices for  $\alpha_\xi(u)$ ,  $\sigma_\xi(u)$ , and  $\tau_\xi(u)$  are given in (de la Kethulle de Ryhove and Mittet, 2012). We utilise this scheme for ABCs at the lateral and bottom boundaries of  $\Omega$ . The top boundary of  $\Omega$ , corresponding to the air-water interface, is handled as in Wang and Hohmann (1993).

### Unconstrained 3D MT inversion utilising time-domain modelling

The properties of an FDTD modelling algorithm can be utilised to obtain a very efficient 3D MT inversion. Specifically, we use the fact that we can compute responses for many frequencies in a single simulation when performing forward or adjoint modelling. For the purpose of minimising the cost function, we utilise the L-BFGS-B optimisation algorithm described by Byrd et al. (1995). A similar optimisation strategy was used by Avdeev and Avdeeva (2009) in combination with integral equation based modelling. The data term of the inversion cost function reads  $\epsilon_{\text{Data}} = \sum_{ij, \omega, n} \left| W_{ij, \omega, n} (Z_{ij, \omega, n}^{\text{Observed}} - Z_{ij, \omega, n}^{\text{Synthetic}}) \right|^2$ .

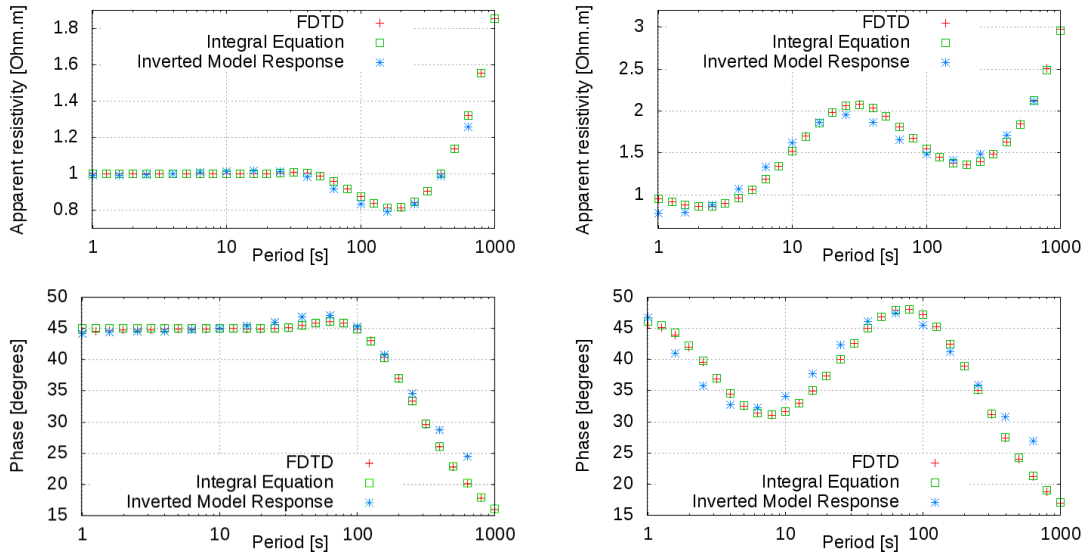


**Figure 2** True model forward response computed by our FDTD scheme, true model forward response computed by integral equation modelling software (for comparison), and inverted model response. The responses are shown for receivers labelled A ( $\rho_{yx}$ ,  $\phi_{yx}$ ; left) and B ( $\rho_{xy}$ ,  $\phi_{xy}$ ; right) in Figure 1.

Here, the indices  $i, j$  denote components of the impedance tensor  $Z$ , and the index  $n$  labels the receivers of the data-set. The quantity  $W_{ij,\omega,n}$  is a weight that is inversely proportional to the datum uncertainty estimated by error propagation.

The forward data determines  $Z^{\text{Synthetic}}$  as well as the forward Green function. This calculation involves two parallel modelling runs for linearly independent directions of the MT source polarisation  $\mathbf{p}$ . The quasi-Newton optimiser also requires that we compute the gradient of  $\mathcal{E}_{\text{Data}}$  w.r.t. the model parameters. In the anisotropic case, the gradient for the horizontal conductivity parameter  $\sigma_V(\mathbf{r})$  can be written

$$\frac{\partial \mathcal{E}_{\text{Data}}}{\partial \sigma_V(\mathbf{r})} = \sum_{l,\omega,\mathbf{p}} \left( \sum_{m,S} G_{lm}^{EE}(\mathbf{r}; \mathbf{r}_S, \omega) J_m(\mathbf{r}_S, \omega) p_m \right) \times \left( \sum_{F,k;n} G_{lk}^{EF}(\mathbf{r}; \mathbf{r}_n, \omega) \mathbf{J}_k^{\mathbf{p},F}(\mathbf{r}_n, \omega) \right) + \text{c.c.} \quad (6)$$

Here,  $G$  denotes tensor Green functions with  $l, m, k$  directional indices to be summed over  $x, y$ . The first parenthesis on the right hand side describes the MT-source generated electric field. The MT source is represented as a uniform current sheet from discretised sources  $J_m$  at all positions  $\mathbf{r}_S$  along the air-water interface. The second factor represents the adjoint state propagation of electric and magnetic  $F \in \{E, H\}$  dipole source contributions with strength  $\mathbf{J}_k^{\mathbf{p},F}(\mathbf{r}_n, \omega)$ . These sources depend on the residuals  $Z_{ij,\omega,n}^{\text{Observed}} - Z_{ij,\omega,n}^{\text{Synthetic}}$  and fields from the forward modelling. Since the sum over receiver sites can be factored out from the contribution of the MT forward sources in equation (6), we can utilise the superposition principle and obtain the adjoint state propagation component from a single modelling run. In summary, each iteration requires two parallel MT forward modelling runs, and two subsequent parallel adjoint modelling runs corresponding to the two polarisations. We emphasise that the computational cost does not scale with the number of receivers or frequencies involved. These properties make the approach numerically very efficient, and suitable for implementation on a single computer.

We inverted synthetic data obtained from the model shown in Figure 1, which consists of a 300  $\Omega\text{m}$  resistive anomaly in a 1D layered earth (0.25  $\Omega\text{m}$  water layer, 1  $\Omega\text{m}$  formation, 100  $\Omega\text{m}$  basement) – and could correspond to a scenario where marine MT data is acquired to image a resistive salt body located above a resistive basement. The water depth is 500 m. The structural imaging problem posed by such model could be highly relevant to enhance seismic imaging and for assessing hydrocarbon prospectivity at salt flanks. For receivers labelled A and B in Figure 1, Figure 2 shows the true model forward response computed using our FDTD scheme, the true model forward response computed using integral equation modelling code (Hursan and Zhdanov, 2002) for comparison, and the inverted model

response. The agreement between the FDTD and integral equation modelling results is excellent. In particular, note that this remains the case (1) for long periods in spite of the fact that the FDTD response for the true model was computed using a modelling grid that is only 10.5 km deep, showing that the CPML ABCs from our FDTD modelling algorithm have performed well; and (2) for receiver A in spite of the proximity of this receiver to the edge of the computational domain, showing that the FDTD modelling results remain accurate even close to the edges of the computational domain.

The initial model for the inversion was a 1  $\Omega\text{m}$  half-space with a total vertical extent of 30 km. Cell spacing in the  $z$ -direction is non-uniform. The upper cells are 100 m thick, while the lowest cell at 30 km is 3 km thick with continuous growth between. In total the model has  $120 \times 120 \times 50$  cells. We inverted the  $xy$ - and  $yx$ -components of the impedance tensor for 100 receivers at 16 frequencies. The inversion took 33 hours using a computer with dual Intel Xeon E5-2690 processors and 256 GB memory. The inverted model agrees structurally with the true model to the expected resolution of the MT data. The lateral extent and the geometry of the salt dome are recovered, specifically the result allows to identify the narrowing structure of the dome. The basement is at approximately the correct depth. The resistivity of the inverted salt dome is lower than in the true model. This is due to the limited sensitivity of MT data to resistive anomalies which can be inferred from the data plots in Figure 2. Although the true salt resistivity is 300  $\Omega\text{m}$ , the effect in apparent resistivity for the true model response at site B over the salt dome is only about 2  $\Omega\text{m}$ . The inverted model responses explain the true model responses quite well.

## Conclusions

We presented an efficient 3D marine MT inversion algorithm based on an original FDTD modelling scheme. Two advantages of the FDTD method over frequency-domain methods are the low memory usage and the fact that single simulations give results for many MT periods. Comparisons to integral equation solutions showed that our algorithm produces accurate modelling results. An inversion example for a marine salt dome model demonstrated the capabilities of our inversion, and indicates how 3D marine MT can aid salt imaging. In future work, we plan to consider integrated solutions combining among others MT, controlled-source electromagnetic, and seismic data for structural imaging applications.

## Acknowledgements

The authors wish to thank EMGS for permission to publish the results, and Rune Mittet and Daniil Shantsev for numerous interesting discussions.

## References

- Avdeev, D. and Avdeeva, A. [2009] 3D magnetotelluric inversion using a limited-memory quasi-Newton optimization. *Geophysics*, **74**, F45–F57.
- Byrd, R.H., Lu, P. and Nocedal, J. [1995] A limited memory algorithm for bound constrained optimization. *SIAM Journal on Scientific and Statistical Computing*, **16**, 1190–1208.
- de la Kethulle de Ryhove, S. and Mittet, R. [2012] Three-dimensional marine magnetotelluric modeling with the finite-difference time-domain method. *Submitted to Geophysics*, 2012.
- Farquharson, C.G. and Miensopust, M.P. [2011] Three-dimensional finite-element modelling of magnetotelluric data with a divergence correction. *Journal of applied Geophysics*, **75**, 699–710.
- Hursan, G. and Zhdanov, M.S. [2002] Contraction integral equation method in three-dimensional electromagnetic modeling. *Radio Science*, **37**, 1089, doi:10.1029/2001RS002513.
- Maaø, F.A. [2007] Fast finite-difference time-domain modeling for marine-subsurface electromagnetic problems. *Geophysics*, **72**, A19–A23.
- Mackie, R.L., Madden, T.R. and Wannamaker, P.E. [1993] Three-dimensional magnetotelluric modeling using difference equations – theory and comparison to integral equation solutions. *Geophysics*, **58**, 215–226.
- Mittet, R. [2010] High-order finite-difference simulations of marine csem surveys using a correspondence principle for wave and diffusion fields. *Geophysics*, **75**, 33–50.
- Roden, J.A. and Gedney, S.D. [2000] Convolutional PML (CPML): An efficient FDTD implementation of the CFS-PML for arbitrary media. *Microwave Optical Tech. Lett.*, **27**, 334–339.
- Sleijpen, G.L.G. and Fokkema, D.R. [1993] BiCGStab(l) for linear equations involving unsymmetric matrices with complex spectrum. *Electro. Trans. Numer. Anal.*, **1**, 11–32.
- Wang, T. and Hohmann, G. [1993] A finite-difference, time-domain solution for three-dimensional electromagnetic modeling. *Geophysics*, **58**, 797–809.
- Yee, K.S. [1966] Numerical solution of initial boundary value problems involving Maxwell's equations in isotropic media. *IEEE Trans. Ant. Prop.*, **AP-14**, 302–307.